九州大学学術情報リポジトリ
Kyushu University Institutional Repository

Laminar Flow Analysis of NACA 4412 Airfoil Through ANSYS Fluent

Muhammad Shehzad Arif
Department of Physics, Government Islamia College

M. Javaid Afzal
Department of Physics, Government Islamia College

Javaid, Farah
Department of Physics, Government APWA College (W) Lahore

Tayyaba, Shahzadi
Department of Computer Engineering, The University of Lahore

他

https://doi.org/10.5109/5909123

出版情報：Proceedings of International Exchange and Innovation Conference on Engineering & Sciences (IEICES). 8, pp.394-399, 2022-10-20. Interdisciplinary Graduate School of Engineering Sciences, Kyushu University
バージョン：
権利関係：Copyright © 2022 IEICES/Kyushu University. All rights reserved.

KYUSHU UNIVERSITY

Proceedings of the 8th International Exchange and Innovation Conference on Engineering & Sciences (IEICES 2022)

Laminar Flow Analysis of NACA 4412 Airfoil Through ANSYS Fluent

Muhammad Shehzad Arif[1], M. Javaid Afzal[1,*], Farah Javaid[2], Shahzadi Tayyaba[3], M. Waseem Ashraf[4], G. F. Ishraque Toki[5], M. Khalid Hossain[6, **]

[1]Department of Physics, Government Islamia College Civil Lines, Lahore 54000, Pakistan
[2]Department of Physics, Government APWA College (W) Lahore, Pakistan
[3]Department of Computer Engineering, The University of Lahore, Lahore 54000, Pakistan
[4]Department of Physics (Electronics), GC University, Lahore 54000, Pakistan
[5]College of Materials Science and Engineering, Donghua University, Shanghai 201620, China
[6]Institute of Electronics, AERE, Bangladesh Atomic Energy Commission, Dhaka 1349, Bangladesh.
Correspondence: *javaidphy@gmail.com , **khalid.baec@gmail.com , khalid@kyudai.jp

Abstract: *Due to the consideration of less angle of attack in the Airfoil, the previous studies didn't achieve accurate results on velocity and pressure of air fluid. Also, previous studies haven't taken into account both the coefficients of drag and lift forces at the same time. In this study, first-time we used the NACA 4412 (national advisory committee for aeronautics 4412) Airfoil because of its availability, lightweight, and flat bottom surface which prevents negative ground effects. Here the NACA 4412 Airfoil surface characteristics were studied through ANSYS Fluent laminar flow analysis as well as pressure-based ANSYS fluent solver. When we increased the angle of attack from 0° to 18° the coefficients of lift and drag forces increase gradually, which impacts the values of the velocity of the upper surface and pressure of the lower surface in the air-fluid. The coefficient of lift and drag forces on the airfoil's surface were 0.44 and 0.5, while the velocity and pressure at the surface are 80.5354 ms^{-1} and 2.12 × 10^3 Pa respectively at a 16° angle.*

Keywords: Aerodynamic; Airfoil; ANSYS fluent; Drag force coefficient; Lift force coefficient.

1. INTRODUCTION

Aerodynamics is the branch of fluid dynamics that deals with the study of the motion of objects through the air [1]. It is the sub-field of fluid dynamics, and gas dynamics [2]. It is also referred to as gas dynamics which deals with the motion of other gases not limited to only the motion of air [3]. The study of aerodynamics in the modern sense started in the 18th century. Later on, the term aerodynamic drag formed the basis of aerodynamics in different technologies of flight. Thus, it is the way objects move through the air [4]. Air is a fluid and by hydrostatical theorem, it is explained as "the pressure exerted by a fluid at equilibrium at any point of time due to force of gravity". So aerodynamic force is produced which is perpendicular and opposite to gravity [5]. So, by the simple understanding of aerodynamic forces, we draw the shape of aircraft moving with the velocity of magnitude V given in Fig. 1 [6].

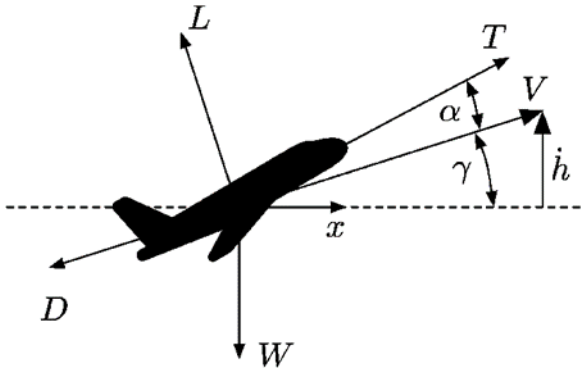

Fig. 1. Component of force and total weight. Reproduced from ref. [6]. Copyright 2022 MDPI.

If we denote the vector by W the weight of the aircraft and by the vector w the force of buoyancy, the total force due to gravity and buoyancy is W + w. We observe that the weight of an aircraft is a force with magnitude W whose direction is vertically downwards, while the force of buoyancy with magnitude w whose direction is vertically upwards so that the magnitude of the resultant force is W- w [7]. This force W + w will act whether the aircraft is at rest or in motion [8]. The aircraft is moving with constant or uniform velocity V in a horizontal direction through the that is at rest, that is to say, any motion of the air is due solely to the motion of the aircraft. This motion is maintained by the tractive force T exerted by the propeller [9]. So, Newton`s first law here is the resultant force exerted on the aircraft or airplanes must be zero, so the motion is decelerated [10]. It follows that there must be an additional force A exerted on this which is the vector sum as in the form of equation (1).

$$T + (W + w) + A = 0 \quad (1)$$

Here, A is denoted as aerodynamic force, which is the force exerted on the airfoil by air due to the relative motion of the airfoil and air [11].

A cross-sectional curved surface shape of a solid object which produces the maximum lift during the motion of that solid object through the air or other gases is called an airfoil. Additionally, it is a curved-surfaced cross-sectional wing that provides the best lift-to-drag relation throughout the flight [12]. A force is made perpendicular to the path of motion by the effect of lift., whereas drag is the factor that makes a force parallel to the direction of motion [13]. The aerodynamic characteristics of the aircraft, in turn, are governed by the aircraft's weight, speed, and intended use. Max Munk, a German mathematician, created the airfoil, which British Aerodynamicists Hermann Blauert and others further improved in 1920 [14]. The NACA 4412 airfoil is used in this work because of its availability, lightweight, and flat bottom surface which prevents negative ground effects. The Bernoulli principle is a single principle that contributes to the understanding of how heavier-than-air objects may fly [15]. It provides a technique to demonstrate that there is a lower pressure above the

airfoil than below. According to Bernoulli's Principle, air that is traveling more slowly has a higher air pressure than air that is moving more quickly [16]. The amount of pressure, or "push," that air particles apply is known as air pressure. This idea aids in our comprehension of how to lift—the capacity to fly—is produced by airplanes. Thus, the lift produced by this principle is defined in Fig. 2 [17].

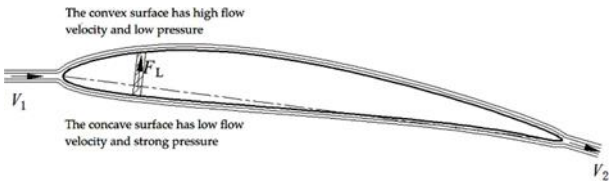

Fig. 2. Bernoulli principle and airfoil with generating lift. Reproduced from ref. [17]. Copyright 2021 MDPI.

A lift is a force that has a component perpendicular to air velocity. The weight of the item is constantly in opposition to aerodynamics [18]. Similar to drag, it is a mechanical force as well, purely controlled by the contact between the aircraft and the fluid. Lift is a force that has both magnitude and direction since it is a vector quantity. Its magnitude is oriented perpendicular to the flow of air and acts through the central pressure of an item. The wing is the primary source of lift [19]. The force that resists an aircraft's passage through the air is called drag which works as a mechanical force. The part of the aerodynamic force called drag acts in the opposite direction to the motion. The interaction and contact of a solid body with the airflow causes this to occur [20]. Always acting in the opposite direction of the motion is the drag force. The total forces acting on the airplane are illustrated in Fig. 3 [21].

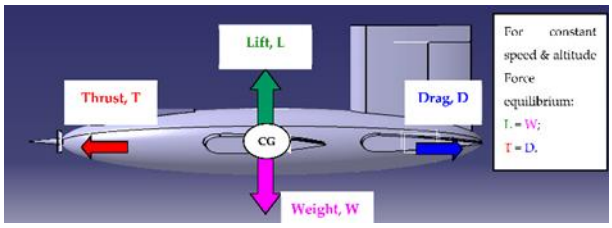

Fig. 3. Forces acting on Aircraft. Reproduced from ref. [21]. Copyright 2021 MDPI.

A dimensionless parameter called the lift coefficient connects a lifting body's lift to the fluid's density, velocity, and matching reference area. A lifting body might be a foil or an entire foil-bearing body, or it can be a fixed-wing aircraft. Mach number, Reynolds number, and the body's tilt to the flow are all important [22]. The lift coefficient is used by aerodynamicists to express all of the complex interactions between shape, tilt, specific flow conditions, and lift. The coefficient of lift (Cl) is defined in the form of equation (2).

$$Cl = \frac{L}{qS} = \frac{2L}{\rho\mu^2 S} \quad (2)$$

Where q denotes the dynamical pressure, which is connected to the fluid density $\boldsymbol{\rho}$, and the flow speed μ. L is the uplift force, and S is the appropriate surface area. the reference surface S selection must be needed for an airfoil to find the coefficient of lift force. For instance, the second axis producing the surface in aerodynamics and thin wing theory is frequently in the chordwise direction, although spirally profiles are always inclined in the spanwise direction.

The drag coefficient, used in fluid dynamics and having no dimensions, measures an object's opposition or drag in a wet environment either air or water [23]. It is utilized in the drag equation, where a lower drag coefficient denotes a reduced amount of aerodynamic or hydrodynamic drag for the item. A specific surface area is constantly linked to the drag coefficient [24]. Any object's drag coefficient combines the effects of form drag and skin friction, the two primary causes of fluid dynamic drag. The impacts of lift-induced drag are also included in the drag coefficient of a rising airfoil or hydrofoil [25]. A full structure, like an airplane, has a drag coefficient that takes interference drag into account as well. The coefficient of drag force (Cd) is defined in the form of equation (3).

$$Cd = \frac{2f_d}{\rho\mu^2 S} \quad (3)$$

Where μ is the flow speed of the item relative to the fluid, $\boldsymbol{\rho}$ is just the mass density of the fluid, and f_d is the drag force, which is, by definition, the force components in the directions of the flow velocity, and the reference area is *A* [26]. The actual wing area serves as the reference area for airfoils. The volume drag coefficient is used by various bodies of revolution and airships, with the reference area being the square of the airship volume's cube root [27]. When two objects that share the same parameter move through a fluid at the same speed, a drag force equivalent to each object's drag coefficient will be applied. These coefficients are frequently used to show how the lift-to-drag ratio changes depending on the angle of attack. With speed, the angle of attack varies depending on the lift's specific magnitude [28]. A wing moves through the air at an angle to the direction of flight. The lift created by a wing is greatly influenced by the angle of attack, while the angle is located in between the chord line and the flight direction. The pilot pushes the plane as hard as possible during takeoff to make it roll down the runway. However, the pilot "rotates" the aircraft immediately before takeoff. The maximum values of lift and drag coefficients are at 16^0 and the minimum value of lift and drag coefficients are at the 0^o angle of attack to generate the lift of an airfoil during the motion of an aircraft. The angle of attack widens and more lift is produced when the aircraft's nose raises, both of which are necessary for takeoff [29]. Now the comparison between the coefficients of lift and drag forces on the surface of an airfoil with different angles of attack that generates the lift during the motion of an aircraft during flight is provided in Table 1.

Different scientists and researchers have found the numerical values of the coefficient of upward lift and backward drag forces for different shapes of airfoils. They found these values for airfoils when an airplane moves in the air. In 2017, S. Obeid et al. evaluated RANS (Renolds averaged Navier-Stokes equations) simulations of the aerodynamic performance of the NACA 0015

flapped airfoil. The numerical findings show that while the lift curve remains constant and just changes upward, greater flap deflections improve the maximum lift coefficient, change the lowest angle of attack values, and minimize stall. Moreover, for a flap deflection of 50^0, the numerical simulations indicate limitations for the lift increments Cl and Cd, with maximum values to be 1.1 and 2.2, respectively with an initial velocity of 50 ms^{-1} and with the pressure of 1.8×10^3 Pa [31]. JVM. Jeyan et al. in 2019, published a computational case study on the aerodynamic characteristics of the NACA 0022 Airfoil, the stall angle is 15º, and the related lift and drag coefficients are 1.4913 and 0.310, respectively. Additionally, experimental data given by NASA was used to verify the Cl, Cd, and coefficient of pressure (Cp) of the NACA-0022 airfoil at a 10º angle of attack. In actuality, Cl was supplied by NASA as 1.1 and Cd as 0.012 for 10º with a pressure of 1.4×10^3 Pa and velocity of 60 ms^{-1} [32]. Chaitanya KK. et al. in 2021 evaluated aerodynamic analysis and optimization of airfoils. The airfoils were examined for a speed of 70 ms^{-1} with a pressure of 1.75×10^3 Pa, at the attack angle of 7°, and up to a maximum Reynolds Number (Re) of 3×10^6. For consistency, the wing chord length was maintained at 1 to 4 m, and the total wing span was at a length of L = 10 m throughout the analysis. In the following study, the top three wings were further revised and interpolated to achieve greater coefficients of lift and drag forces, which were 0.41 and 0.55, respectively [33]. Many research groups have used ANSYS Fluent to simulate the different parameters of air-fluid for different types of airfoils. But they used only 7º and 10º angles of attack and only used either the coefficients of drag or coefficients of lift forces for values of pressure and velocity of an air fluid, which had less accuracy concerning expected results.

Table 1. Comparison of coefficients [30].

Angle of attack	Lift coefficient	Drag coefficient
0	-0.000401	0.009239
4	0.449270	0.010800
6	0.670040	0.012887
8	0.883000	0.015914
10	1.071900	0.019906
12	1.261900	0.026041
14	1.407400	0.034709
16	1.467800	0.050969
17	1.395900	0.071730
18	1.082600	0.148530

In this simulation work, we have studied the laminar flow analysis of air-fluid for NACA 4412 airfoil through ANSYS fluent to simulate the values of pressure and velocity of air-fluid for the very first time. We have used NACA 4412 airfoil because of its large volume of applications in aircraft, lightweight, and flat bottom surface which prevents negative ground effects. During the study, the coefficient of lift and drag, the velocity of the upper surface, and the pressure of the lower surface of air-fluid for the airfoil are determined from 0º to 18º angles of attack.

2. ANSYS SIMULATION

ANSYS is a very popular software around the world for Multiphysics and engineering simulations. Many researchers have used ANSYS software for simulation fabrication [34,35,44,45,36–43]. For real-time simulations, ANSYS has become an amazingly powerful piece of software nowadays. In this study, we have used the ANSYS fluent for the laminar flow analysis of air-fluid to find the coefficients of lift and drag forces for the NACA 4412 airfoil. The geometry of the NACA 4412 airfoil is designed with the dimension of 1 m chord length. The area and volume of the surface of the NACA 4412 airfoil are 445.22 m^2 and 543.19 m^3 respectively. The enclosure of 6 m, 3 m, 3 m, 5 m, 3 m, and 3 m lengths respectively has been drawn to get a better result of fluid moving around the symmetrical surface of the airfoil of an aircraft as shown in Fig. 4.

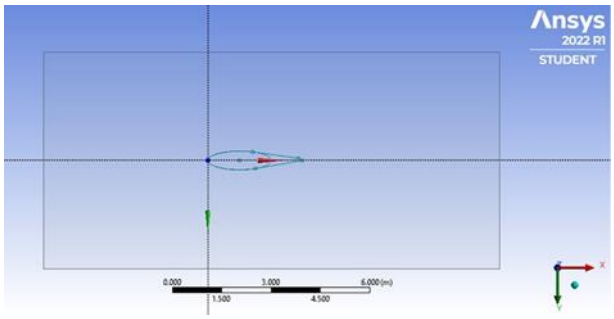

Fig. 4. Geometry of an Airfoil.

An airfoil's shape has been meticulously meshed for accurate simulation, with each domain's element size set at 0.25 mm. All the parts of the NACA 4412 airfoil are specified in the meshing step while computational fluid dynamics (CFD) meshing was used. The inlet, outlet, and walls of the NACA 4412 airfoil are named in this step. The geometry of the elements and nodes is maintained in a triangle form, and the meshing configuration includes medium smoothing, coarse relevance center, and these features. There are 427101 total elements and 76594 total nodes in the mesh geometry reflected in Fig. 5.

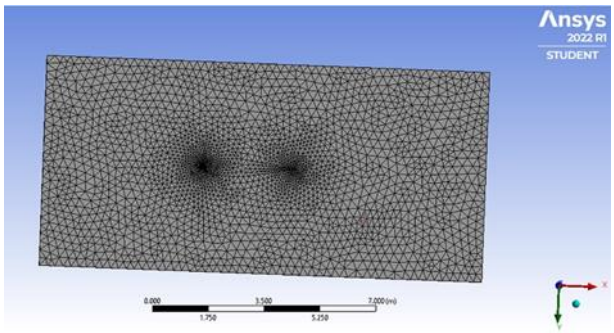

Fig. 5. Meshing of an Airfoil.

The next step is solution setup, in this step, we select the fluid which is air here, and the viscous laminar model for the flow of air-fluid to get better results from the simulation. In boundary conditions, the inlet is taken as inlet velocity with an initial value of 60 ms^{-1} and outlets as outlet pressure. Pressure-based ANSYS fluent solver, absolute velocity formulation, and steady time are used in solution setup to perform the calculation. Then we

determined the coefficients of lift and drag forces in the report definition process by creating their respective names and selecting the airfoil wing portion only. Finally, we initialized the all-zones values.

3. RESULT AND DISCUSSION

The graph of the coefficient of lift force by running the calculation to compare with different angles of attack is drawn (Fig. 6). The maximum value of the coefficient of the lift force is -800 at a 0º angle of attack then gradually decreases to 2700 at 10º. The coefficient of lift force again rapidly increases for the next angles of attack gradually as shown in Fig. 6.

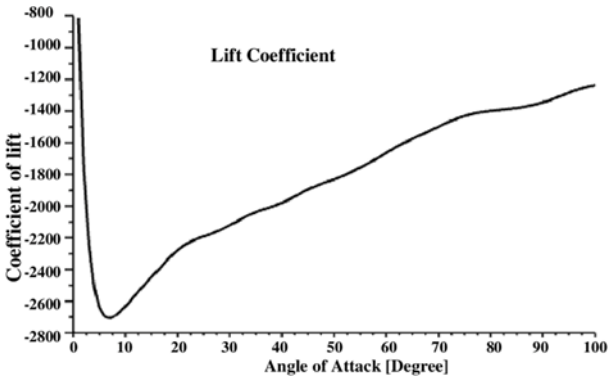

Fig. 6. Coefficient of lift plot

The graph of the coefficient of the drag force to compare with different angles of attack is drawn in this simulation (Fig. 7). We have observed that the maximum value of the coefficient of drag is 8000 at 0º which decreases to 1000 at 10º. The value of the coefficient of lift does not change with the next angles of attack illustrated in Fig. 7.

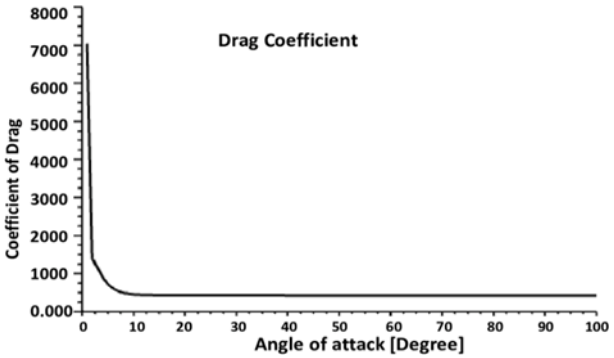

Fig. 7. Graph of drag coefficient.

The graph between the static pressure and length of the airfoil wing on the surface of an airfoil is drawn through ANSYS fluent (Fig. 8). The air pressure 2.12×10^3 Pa exerted on the lower surface of NACA 4412 airfoil at the center is the maximum at 1.5 m length of chord line whereas the low pressure of 110 Pa is exerted on the top surface of an airfoil given in Fig. 8.

For ANSYS fluent simulation, the NACA 4412 airfoil is designed with the initial velocity of 60 ms^{-1} as an input variable to compute the values of coefficient of lift and drag forces by naming them in the report definition in ANSYS fluent setup for laminar flow of air-fluid which is 0.44 and 0.51, respectively for 100 iterations. The value of fluid velocity for the airfoil is 80.5354 ms^{-1} means that air is moving with the velocity of 80.5354 ms^{-1} around the surface of an airfoil and it's all its domains are shown in Fig. 9.

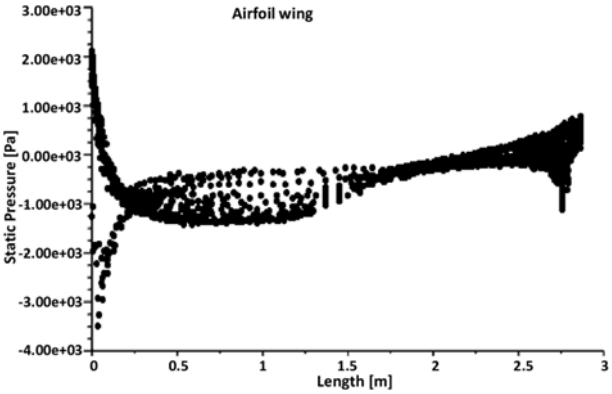

Fig. 8. Graph of static pressure.

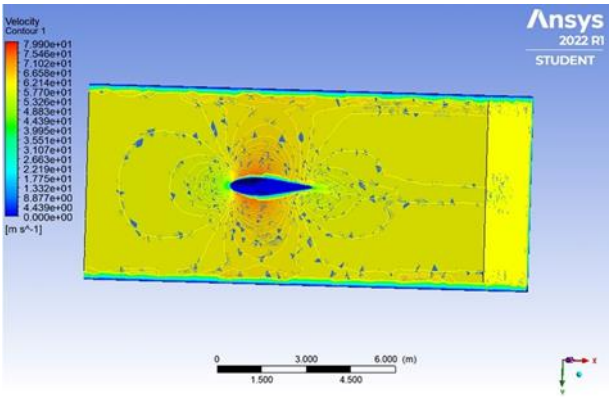

Fig. 9. Velocity contour mapping.

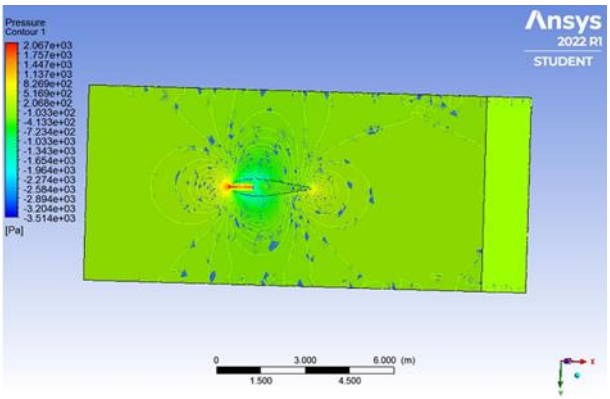

Fig. 10. Pressure contour mapping.

The air exerts a pressure of 2.12×10^3 Pa on the surface of an airfoil and it's all the domains are called the pressure outlet pressure. Many researchers, including S. Obeid et al. (2017), JVM. Jeyan et al. (2019), and Chaitanya KK et al. (2021), have used ANSYS simulation to determine the coefficients of lift and drag forces, which are 1.1, 2.2, 0.31, 0.41, and 0.51 with the pressure of 1.8×10^3 Pa, 1.4×10^3 Pa, 1.75×10^3 Pa includes velocities of 50 ms^{-1}, 60 ms^{-1}, 70 ms^{-1} around the surface of an airfoil respectively. At the upper and lower surfaces of the airfoil, the airflow is moving at a velocity of 80.5354 ms^{-1} and a pressure of 2.12×10^3 Pa. We can more precisely calculate the airflow's velocity and pressure with an angle of attack elevation of 16º. This result shows excellent agreement with standard simulation. These all are designed output

variables for an airfoil through ANSYS fluent as illustrated in Fig. 10.

As the relation between the pressure is inverse to each other so where the pressure is high, velocity will be low at that point and vice versa. We have observed that the air-fluid is moving with a high speed of 80.5354 ms^{-1} on the upper surface of an airfoil with a low pressure of 110 Pa whereas at the lower surface of an airfoil a high pressure of 2.12×10^3 Pa is exerted with a low velocity of 35 ms^{-1}. And the graph between the pressure and velocity of air moving around the surface of the NACA 4412 airfoil is given in Fig. 11.

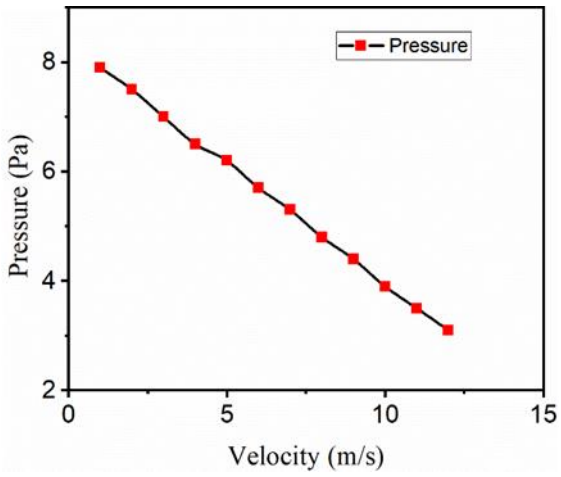

Fig. 11. Graph between pressure and velocity.

Fig. 11 shows the inverse relation of velocity and pressure according to the Bernoulli principle. The air exerts low pressure of 110 Pa on the upper surface of the NACA 4412 airfoil and high pressure of 2.12×10^3 Pa on the lower surface whereas the air moves with a velocity of 80.5354 ms^{-1} on the upper surface and moves slower with a velocity of 35 ms^{-1} at a lower surface of an airfoil which helps to generate maximum upward lift 88. 97 N for an airfoil during the motion of an airplane in flight.

4. CONCLUSION

This study provides a precise method of using ANSYS Fluent to examine the coefficients of lift and drag forces, velocity, and pressure on the surface of the NACA 4412 airfoil. During the simulation, the coefficients of lift and drag forces were 0.44 and 0.51, respectively, while the coefficients of an airfoil generate the maximum lift force of 88.97 N during the motion of an airplane. Thus, the velocity of the air-fluid acting on the upper surface of the NACA 4412 airfoil is 80.5354 ms^{-1}. The air exerts a pressure of 2.12×10^3 Pa on the lower surface of the airfoil which is more significant than in the previously reported results. Furthermore, for NACA 4412 airfoil, impressive accuracy has been achieved, while the pressure on the airfoil's bottom surface of 2.12×10^3 Pa and the velocity of air entering the inlet of 80.5354 ms^{-1}, the maximum lift of 88.97 N is generated at 16º. This work could help the next studies to get the more precise values of pressure and velocity of air-fluid to generate maximum lift at ≥10º angles for more efficient and supersonic aircraft in the future. If both the coefficients of lift and drag forces are used together, a better result of velocity, pressure and a maximum lift of air-fluid could be achieved which may also accelerate further similar studies.

5. REFERENCES

[1] JS Wong, Aerodynamic study of a new car roof box using CFD, Univ. Tek. Malaysia Melaka. (2021).

[2] C. Zheng, Z. Wang, J. Zhang, Y. Wu, Z. Jin, Y. Chen, Effect of the combined aerodynamic control on the amplitude characteristics of wind loads on a tall building, Eng. Struct. 245 (2021) 112967.

[3] C. Larriba-Andaluz, F. Carbone, The size-mobility relationship of ions, aerosols, and other charged particle matter., J. Aerosol Sci. 151 (2021) 105659.

[4] M. Drela, Considerations in Aerodynamic Force Decomposition, in: AIAA Aviat. 2021 Forum, American Institute of Aeronautics and Astronautics, Reston, Virginia, Virginia, 2021. https://doi.org/10.2514/6.2021-2552.

[5] S. Jayapregasham, Effect of Varying Reynolds Number On The Aerodynamic Design of Lifting Surfaces, (n.d.) 1–7.

[6] J.P. Jasa, B.J. Brelje, J.S. Gray, C.A. Mader, J.R.R.A. Martins, Large-Scale Path-Dependent Optimization of Supersonic Aircraft, Aerospace. 7 (2020) 152.

[7] T.-H. Liu, L. Wang, Z.-W. Chen, H.-R. Gao, W.-H. Li, Z. Guo, Y.-T. Xia, X.-S. Huo, Y.-W. Wang, Study on the pressure pipe length in train aerodynamic tests and its applications in crosswinds, J. Wind Eng. Ind. Aerodyn. 220 (2022) 104880.

[8] A. Karthik, D.S. Chiniwar, M. Das, P. Pai M, P. Prabhu, P.A. Mulimani, K. Samanth, N. Naik, Electric Propulsion for Fixed Wing Aircrafts – A Review on Classifications, Designs, and Challenges, Eng. Sci. (2021).

[9] T. Ullah, K. Sobczak, G. Liśkiewicz, A. Khan, Two-Dimensional URANS Numerical Investigation of Critical Parameters on a Pitch Oscillating VAWT Airfoil under Dynamic Stall, Energies. 15 (2022) 5625.

[10] E.J. Limacher, Added-mass force on elliptic airfoils, J. Fluid Mech. 926 (2021) R2.

[11] J. Zhang, Z. Lv, H. Hua, C. Zhang, H. Yu, Y. Jiao, Numerical Study of the Fish-like Robot Swimming in Fluid with High Reynolds Number: Immersed Boundary Method, Actuators. 11 (2022) 158.

[12] K. Asai, P.S. John, E. Yasuhiro, C. Klein, Pressure and Temperature Sensitive Paints Second Edition, n.d.

[13] J.D. Tank, B.F. Klose, G.B. Jacobs, G.R. Spedding, Flow transitions on a cambered airfoil at moderate Reynolds number, Phys. Fluids. 33 (2021) 093105.

[14] M. Moriche, G. Sedky, A.R. Jones, O. Flores, M. García-Villalba, Characterization of Aerodynamic Forces on Wings in Plunge Maneuvers, AIAA J. 59 (2021) 751–762.

[15] M.A. Akimov, A.D. Budovskiy, A.D. Obuhovskiy, P.A. Polivanov, Experimental and numerical study of the aerodynamic drag crisis phenomenon of a symmetrical thick teardrop airfoil with rounded trailing edge, in: 2021: p. 040013.

[16] S. Shao, Z. Guo, Z. Hou, G. Jia, L. Zhang, X.

Gao, Effects of Coanda jet direction on the aerodynamics and flow physics of the swept circulation control wing, Proc. Inst. Mech. Eng. Part G J. Aerosp. Eng. (2022) 095441002110687.
[17] C. Jiang, X. Shu, J. Chen, L. Bao, Y. Xu, Research on Blade Design of Lift–Drag-Composite Tidal-Energy Turbine at Low Flow Velocity, Energies. 14 (2021) 4258.
[18] H. Hessenkemper, T. Ziegenhein, R. Rzehak, D. Lucas, A. Tomiyama, Lift force coefficient of ellipsoidal single bubbles in water, Int. J. Multiph. Flow. 138 (2021) 103587.
[19] A. Guilarte Herrero, A. Noguchi, K. Kusama, T. Shigeta, T. Nagata, T. Nonomura, K. Asai, Effects of compressibility and Reynolds number on the aerodynamics of a simplified corrugated airfoil, Exp. Fluids. 62 (2021) 63.
[20] N. Hosseini, M. Tadjfar, A. Abba, Numerical Study of Aerodynamic Forces of Two Airfoils in Tandem Configuration at Low Reynolds Number, in: Vol. 3 Fluid Mech. Micro Nano Fluid Dyn. Multiph. Flow, American Society of Mechanical Engineers, 2021.
[21] I.-M. Ghiţescu, M.L. Scutaru, M. Ghiţescu, P.N. Borza, M. Marin, New Command Mechanism of Flaps and Wings of a Light Sport Aircraft, Symmetry (Basel). 13 (2021) 221.
[22] D. Wang, Q. Lin, C. Zhou, J. Wu, Aerodynamic performance of a self-propelled airfoil with a non-zero angle of attack, Phys. Fluids. 34 (2022) 031901.
[23] D. Kumar, A.K. Sahu, Non-Newtonian fluid flow over a rotating elliptic cylinder in laminar flow regime, Eur. J. Mech. - B/Fluids. 93 (2022) 117–136.
[24] N. Poudel, M. Yu, J.T. Hrynuk, Gust mitigation with an oscillating airfoil at low Reynolds number, Phys. Fluids. 33 (2021) 101905.
[25] A. Lu, T. Lee, Effect of Ground Boundary Condition on Near-Field Wingtip Vortex Flow and Lift-Induced Drag, J. Fluids Eng. 143 (2021).
[26] I.G. Kartana, Anak Agung Adhi Suryanwan, I Gusti Ketut Sukadana, Simulation of Airflow Patterns and Aerodynamic Forces on a Chambered Airfoil and Symmetric Airfoil with Maximum Thickness Variation, Nat. Sci. Eng. Technol. J. 3 (2022) 148–159.
[27] M.S.B.M. Shahid, study of F1 car aerodynamic rear wing using computational fluid dynamic (CFD), Univ. Malaysia Pahang. 1 (2020) 274–282.
[28] K. Szwedziak, T. Łusiak, R. Bąbel, P. Winiarski, S. Podsędek, P. Doležal, G. Niedbała, Wind Tunnel Experiments on an Aircraft Model Fabricated Using a 3D Printing Technique, J. Manuf. Mater. Process. 6 (2022) 12.
[29] P. Tanjung, Computational Fluid Dynamics Notes: Fundamentals of Fluid Dynamics, SSRN Electron. J. (2021).
[30] C. Vourtsis, W. Stewart, D. Floreano, Robotic Elytra: Insect-Inspired Protective Wings for Resilient and Multi-Modal Drones, IEEE Robot. Autom. Lett. 7 (2022) 223–230.
[31] S. Obeid, R. Jha, G. Ahmadi, RANS Simulations of Aerodynamic Performance of NACA 0015 Flapped Airfoil, Fluids. 2 (2017) 2.
[32] C. Bilji, J. V Muruga, L. Jeyan, A Computational Case Study on Aerodynamic parameters of NACA 0022 Aerofoil, (2019) 37–45.
[33] K.K. Chaitanyaa, C.R. Patil, B. Pal, D. Dandotiya, Aerodynamic Analysis and Optimization of Airfoils Using Vortex Lattice Method, IOP Conf. Ser. Mater. Sci. Eng. 1013 (2021) 012023.
[34] Muhammad Javaid Afzal; Muhammad Waseem Ashraf; Shahzadi Tayyaba; Akhtar Hussain Jalbani; Farah Javaid, Computer simulation based optimization of aspect ratio for micro and nanochannels, Mehran Univ. Res. J. Eng. Technol. 39 (2020) 779–791.
[35] M. Afzal, M. Ashraf, S. Tayyaba, M.K. Hossain, N. Afzulpurkar, Sinusoidal Microchannel with Descending Curves for Varicose Veins Implantation, Micromachines. 9 (2018) 59.
[36] M.J. Afzal, F. Javaid, S. Tayyaba, M.W. Ashraf, M.K. Hossain, Study on the Induced Voltage in Piezoelectric Smart Material (PZT) Using ANSYS Electric & Fuzzy Logic, Proc. Int. Exch. Innov. Conf. Eng. Sci. 6 (2020) 313–318.
[37] M.J. Afzal, F. Javaid, S. Tayyaba, M.W. Ashraf, C. Punyasai, N. Afzulpurkar, Study of Charging the Smart Phone by Human Movements by Using MATLAB Fuzzy Technique, in: 2018 15th Int. Conf. Electr. Eng. Comput. Telecommun. Inf. Technol., IEEE, 2018: pp. 411–414.
[38] and M.I.Y. M. J. Afzal, F. Javaid, S. Tayyaba, M. W. Ashraf, Study of Constricted Blood Vessels through ANSYS Fluent, Biologia (Bratisl). 66 (2020) 197–201.
[39] and M.W.A. M. J. Afzal, F. Javaid, S. Tayyaba, A. Sabah, Fluidic simulation for blood flow in five curved Spiral Microchannel, Biologia (Bratisl). 65 (2019) 141.
[40] M.J. Afzal, S. Tayyaba, Fazal-e-Aleem, M.W. Ashraf, M.K. Hossain, N. Afzulpurkar, Fluidic simulation and analysis of spiral, U-shape and curvilinear nano channels for biomedical application, in: 2017 IEEE Int. Conf. Manip. Manuf. Meas. Nanoscale, IEEE, 2017: pp. 190–194.
[41] M. Afzal, S. Tayyaba, M. Ashraf, M.K. Hossain, M. Uddin, N. Afzulpurkar, Simulation, Fabrication and Analysis of Silver Based Ascending Sinusoidal Microchannel (ASMC) for Implant of Varicose Veins, Micromachines. 8 (2017) 278.
[42] M.J. Afzal, S. Tayyaba, M.W. Ashraf, G. Sarwar, Simulation of fuzzy based flow controller in ascending sinusoidal microchannels, in: 2016 2nd Int. Conf. Robot. Artif. Intell., IEEE, 2016: pp. 141–146.
[43] A. Ismaiel, S. Yoshida, Aeroelastic Analysis of a Coplanar Twin-Rotor Wind Turbine, Energies. 12 (2019) 1881. https://doi.org/10.3390/en12101881.
[44] Preeti Verma, Multi Rotor Wind Turbine Design And Cost Scaling, Univ. Massachusetts Amherst. (2013).
[45] M.T. Khan, M.J. Afzal, F. Javaid, S. Tayyaba, M.W. Ashraf, M.K. Hossain, Study of Tip Deflection on a Copper-Steel bimetallic Strip by Fuzzy Logic and ANSYS Static Structural, Proc. Int. Exch. Innov. Conf. Eng. Sci. 7 (2021) 255–260.